

TA7
W34
no. S-78-4
Cop. 2

US-CE-C Property of the United States Government



TECHNICAL REPORT S-78-4

DEPTH AND MOTION PREDICTION FOR EARTH PENETRATORS

by

Robert S. Bernard

Soils and Pavements Laboratory
U. S. Army Engineer Waterways Experiment Station
P. O. Box 631, Vicksburg, Miss. 39180

June 1978

Final Report

Approved For Public Release; Distribution Unlimited



Prepared for Office, Chief of Engineers, U. S. Army
Washington, D. C. 20314

Under Project 4A161102AT22
Task A2, Work Unit 06

LIBRARY BRANCH
TECHNICAL INFORMATION CENTER
US ARMY ENGINEER WATERWAYS EXPERIMENT STATION
VICKSBURG, MISSISSIPPI

PREFACE

The investigation reported herein was conducted for the Office, Chief of Engineers, U. S. Army, by personnel of the Soil Dynamics Division (SDD), Soils and Pavements Laboratory (S&PL), U. S. Army Engineer Waterways Experiment Station (WES), as a part of Project 4A161102AT22, Task A2, Work Unit 06, "Effectiveness of Earth Penetrators in Various Geologic Environments."

Mr. R. S. Bernard conducted the research during the period October 1977-January 1978 with the technical guidance of Dr. B. Rohani and under the supervision of Dr. J. G. Jackson, Jr., Chief, SDD, and Messrs. J. P. Sale and R. G. Ahlvin, Chief and Assistant Chief, S&PL, respectively. This report was also prepared by Mr. Bernard.

COL J. L. Cannon, CE, was Director of WES throughout the investigation and during the preparation of the report. Mr. F. R. Brown was Technical Director.

CONTENTS

	<u>Page</u>
PREFACE	1
PART I: INTRODUCTION	3
Background	3
Purpose	7
Scope	7
PART II: SOIL PENETRATION ANALYSIS	8
PART III: ROCK PENETRATION ANALYSIS	16
PART IV: LAYERED TARGET ANALYSIS	21
Equation of Motion for Layered Targets	21
Layered Soil Targets	21
Layered Rock Targets	23
Composite Targets	24
PART V: CONCLUSIONS	26
REFERENCES	27
APPENDIX A: NOTATION	A1

DEPTH AND MOTION PREDICTION FOR EARTH PENETRATORS

PART I: INTRODUCTION

Background

1. Earth-penetrating weapons (EPW's) offer a means of reducing collateral effects in the selective destruction of localized targets (airfields, factories, utilities, etc.). The effectiveness of these weapons, however, is contingent upon (a) accurate delivery, (b) impact survival, and (c) proper depth-of-burst (DOB). The first two requirements are obvious; the last is important because there is an optimum DOB in the trade-off between destructive capability and collateral effects. To guarantee detonation at or near the optimum DOB, it is necessary to be able to predict the subsurface motion of an EPW.

2. There are three alternatives for predicting EPW-motion after impact: (a) two-dimensional finite-difference codes, (b) equations of motion based partly on theory, and (c) empirical formulae. Alternative (a) is acceptable in some cases but is too expensive for general application. Alternatives (b) and (c) require far less computation and are therefore suitable for parameter studies and multiple predictions.

3. Among the theoretically based equations of motion, those developed from the Cavity Expansion Theory (CET)¹⁻³ have been preferred at the U. S. Army Engineer Waterways Experiment Station. Of the purely empirical formulae, Young's equation⁴⁻⁶ seems now to be the most widely accepted for calculating final penetration depth in soil. The main difference between these two approaches lies in the target description. The CET-based analysis calculates penetration resistance in terms of the mechanical properties of the target (density, strength, elasticity, and compressibility). Young's equation, on the other hand, employs a single empirical parameter (S) to quantify the target penetrability:

$$Z = 0.607 \text{ KSN} \sqrt{\frac{W}{A}} \ln \left(1 + \frac{V^2}{4650} \right), \quad V < 61 \text{ m/sec} \quad (1)$$

$$Z = 0.0117 KSN \sqrt{\frac{W}{A}} (V - 30.5) , V \geq 61 \text{ m/sec} \quad (2)$$

where

Z = final penetration depth, m

K = mass-scaling factor, dimensionless*

S = soil penetrability index, dimensionless**

N = projectile nose-performance coefficient, dimensionless†

W = projectile weight, kg

A = projectile cross-sectional area, cm²

V = projectile impact velocity, m/sec

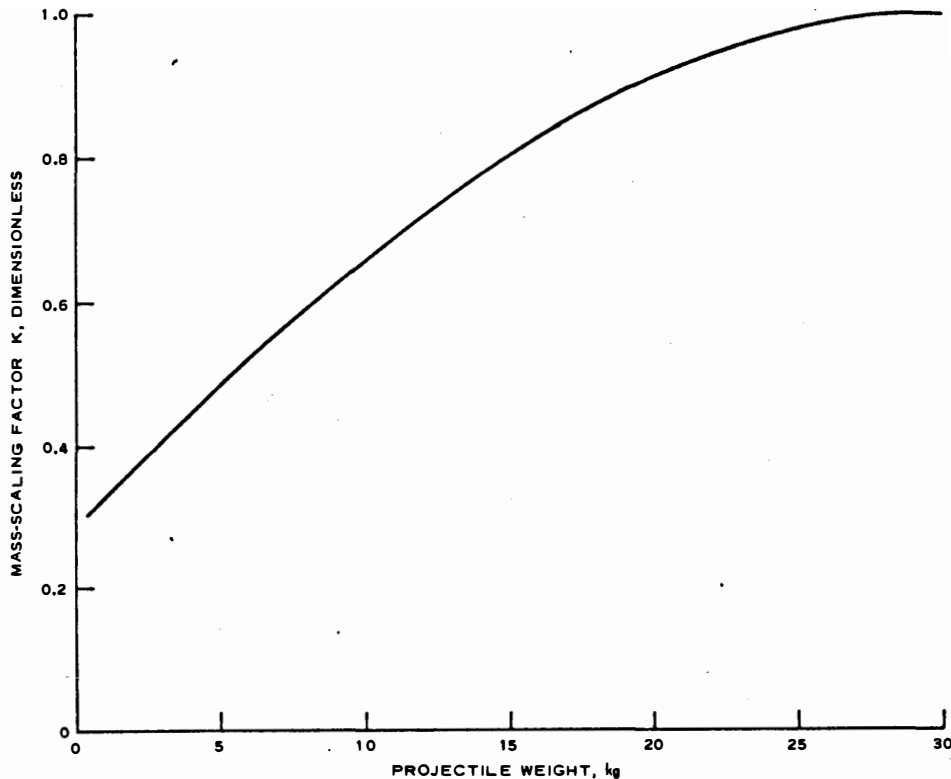


Figure 1. Young's mass-scaling factor for Equations 1 and 2

* The mass-scaling factor is unity for $W > 27$ kg. Figure 1 shows a plot of K versus W for $W \leq 27$ kg.

** Table 1 lists S-values for several types of soil.

† Table 2 lists N-values for various nose shapes.

Table 1*

Typical S-Numbers for Natural Earth Materials

S	Materials
0.2-1	Massive medium- to high-strength rock, with few fractures. Concrete, 2000 to 5000 psi, reinforced.
1-2	Frozen silt or clay, saturated, very hard. Rock, weathered, low strength, fractured. Sea or freshwater ice more than 10 feet thick.
2-3	Massive gypsite deposits (WSMR**). Well-cemented coarse sand and gravel. Caliche, dry. Frozen moist silt or clay.
4-6	Sea or freshwater ice from 1 to 3 feet thick. Medium dense, medium to coarse sand, no cementation, wet or dry. Hard, dry dense silt or clay (TTR† dry lake playas). Desert alluvium.
8-12	Very loose fine sand, excluding topsoil. Moist stiff clay or silt, medium dense, less than about 50 percent sand.
10-15	Moist topsoil, loose, with some clay or silt. Moist medium stiff clay, medium dense, with some sand.
20-30	Loose moist topsoil with humus material, mostly sand and silt. Moist to wet clay, soft, low shear strength.
40-50	Very loose dry sandy topsoil (Eglin AFB). Saturated very soft clay and silts, with very low shear strengths and high plasticity. (Great Salt Lake Desert and bay mud at Skaggs Island.) Wet lateritic clays.

* Taken from Reference 6.

** White Sands Missile Range, New Mexico.

† Tonopah Test Range, Nevada.

Table 2*

Nose Performance Coefficient

<u>Nose Shape</u>	<u>Nose Length-to-Diameter Ratio (L/D)</u>	<u>N</u>
Flat	0	0.56
Hemisphere	0.5	0.65
Cone	1	0.82
Tangent ogive**	1.4	0.82
Tangent ogive	2	0.92
Tangent ogive	2.4	1.0
Inverse ogive	2	1.03
Cone	2	1.08
Tangent ogive	3	1.11
Tangent ogive	3.5	1.19
Step cone	3	1.28
Biconic	3	1.31
Inverse ogive	3	1.32
Cone	3	1.33

* Taken from Reference 6.

** For tangent ogives, L/D is related to the caliber radius (CRH) by

$$CRH = L^2/D^2 + 1/4 .$$

4. A recent study by Rohani et al.⁷ has shown that, for inaccessible targets, analysts with different backgrounds are more likely to agree upon S-number estimates than upon mechanical-property estimates. Equating analyst agreement with reduced uncertainty of prediction, Young's equation is apparently better suited for inaccessible targets than is the CET analysis. This value judgement does not necessarily apply for accessible targets, where S-numbers and mechanical properties can be determined by experiment.

5. Young's equation has been fairly well validated for soil, but its applicability is questionable for hard materials, such as concrete and rock. In fact, penetration data for concrete⁸ indicate that the final depth is more nearly proportional to W/A than to $\sqrt{W/A}$. This seems to warrant a composite prediction technique, with distinct analyses for soil and rock (or rocklike materials).

Purpose

6. An improved method of earth-penetration analysis is sought, particularly for inaccessible targets. A projectile equation of motion will be formulated for soil, retaining Young's S-number and approximately reproducing Young's final-depth equation after integration. A distinct equation of motion will be developed for rock, using density, unconfined compressive strength, and Rock Quality Designation (RQD)⁹ to describe the target. The two analyses will then be interfaced in a composite analysis for targets containing both soil and rock layers.

Scope

7. Part II contains the soil penetration analysis, and Part III the rock penetration analysis. Equations for layered targets are developed in Part IV. Part V states the conclusions drawn from the investigation.

PART II: SOIL PENETRATION ANALYSIS

8. In soil penetration tests conducted with instrumented projectiles, the deceleration curve-shape most often observed is approximately that of a "square pulse."⁶ In targets with distinct soil layers, the deceleration record is usually a series of two or more square pulses, as shown in Figure 2 (taken from Reference 10).^{*} The magnitude of the deceleration is velocity dependent;⁶ an increase in the impact velocity usually causes a proportionate increase in the deceleration level.

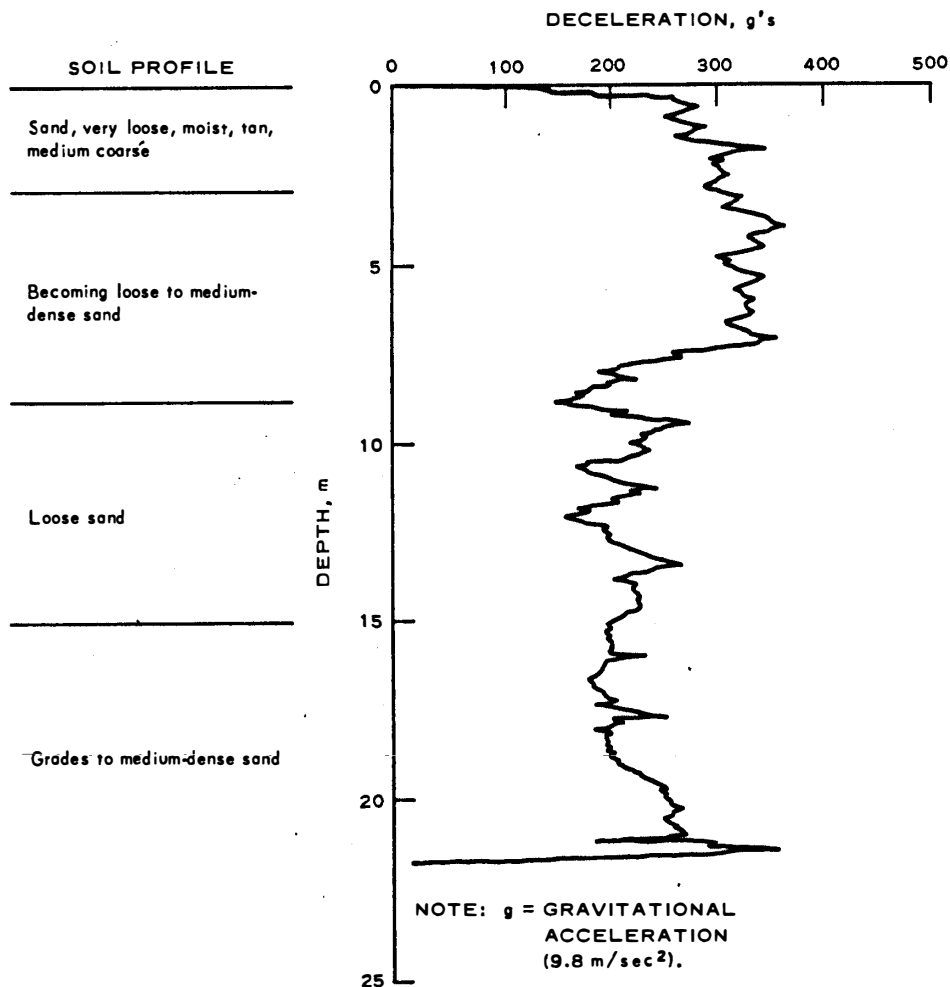


Figure 2. Measured deceleration record in moist sand

* The oscillations in the record are thought to arise from the projectile nonrigidity and from the accelerometer mountings themselves.

9. In order to be generally consistent with experimental data, the projectile equation of motion must (a) exhibit velocity dependence and (b) generate flat deceleration records* in uniform targets. The simplest equation of motion that can satisfy both criteria is

$$-M \frac{dv}{dt} = -Mv \frac{dv}{dz} = bv + cz \quad (3)$$

where

M = projectile mass

v = instantaneous velocity

t = time

z = instantaneous depth

b, c = coefficients dependent on soil type and projectile parameters but independent of velocity and depth

The initial conditions for Equation 3 are $v = V$ and $z = 0$; the final conditions are $v = 0$ and $z = Z$.

10. Disregarding any change in load during the nose-embedment process, Equation 3 is integrated with respect to z , obtaining the following expression:

$$MV^2 = cZ^2 + 2b \int_{z=0}^{z=Z} v \, dz \quad (4)$$

It can be shown that if dv/dt is approximately constant between $z = 0$ and $z = Z$; then Equation 4 reduces to

$$MV^2 \approx cZ^2 + \frac{4}{3} bVZ \quad (5)$$

Thus, the expression for the final penetration depth becomes

$$Z \approx \frac{V}{c} \left(-\frac{2}{3} b + \sqrt{\frac{4}{9} b^2 + Mc} \right) \quad (6)$$

* "Flat" in the sense that the deceleration is essentially constant after nose embedment.

Since the deceleration curve is nearly flat, the initial deceleration (at $z = 0$) is about equal to the final deceleration (at $v = 0$), i.e.,

$$bV \approx cZ \quad (7)$$

Combining Equations 6 and 7 to eliminate V and Z , it follows that

$$b \approx -\frac{2}{3}b + \sqrt{\frac{4}{9}b^2 + Mc} \quad (8)$$

Upon rearranging and squaring both sides of Equation 8, a simple relation occurs between b and c :

$$b^2 \approx \frac{3}{7}Mc \quad (9)$$

Equation 9 reveals that b and c are not independent; b is proportional to the square root of the projectile mass:

$$b \approx \sqrt{\frac{3}{7}Mc} \quad (10)$$

Thus, the presumption of a flat deceleration curve requires that b depend on M , while c remains independent of M .*

11. Sandia Laboratories has conducted at least 47 low-speed penetration tests ($V < 80$ m/sec) in the TTR Main Lake area.¹¹ In 43 of these tests, the projectiles had nearly the same mass (100 to 105 kg), with different diameters and nose shapes. The trends in the TTR data (and likewise in Young's equation) can be summarized as follows:

- a. The relation between final depth (Z) and impact velocity (V) is nonlinear when V is significantly less than 60 m/sec.

* It might be argued that M should appear only on the left-hand side of the projectile equation of motion (Equation 3). The presumption of a flat deceleration curve at the outset, however, forces M to appear on the right-hand side in the velocity coefficient b . No additional interpretation can be given to the mass dependence of b without explaining why the deceleration curve is flat in the first place.

- b. The final depth is inversely proportional to the projectile diameter (D).
- c. The final depth is a function of the projectile nose shape.

The nonlinear relation between Z and V at low speed suggests that the equation of motion needs an additional constant term:

$$-M \frac{dv}{dt} = -Mv \frac{dv}{dz} = a + bv + cz \quad (11)$$

With this modification the deceleration curve still remains flat, and Equation 11 can be solved for the final depth in the same way as Equation 3. The solution obtained is

$$Z \approx \frac{1}{c} \left[-\left(a + \frac{2}{3} bV\right) + \sqrt{\left(a + \frac{2}{3} bV\right)^2 + McV^2} \right] \quad (12)$$

Assuming that Z is inversely proportional to D and directly proportional to N and S, it follows from Equations 10 and 12 that

$$a = \frac{\alpha D}{SN} \quad (13)$$

$$b = \frac{D}{SN} \sqrt{\frac{3}{7} \beta M} \quad (14)$$

$$c = \frac{\beta D^2}{S^2 N^2} \quad (15)$$

where α and β are "universal" constants, independent of projectile parameters and soil properties.

12. Up to this point, the analysis has dealt only with generalities, establishing the form of the equation of motion (Equation 11) and the resulting form of the final-depth equation (Equation 12). The nose-performance coefficient (N) and the penetrability index (S) have been retained for consistency with Young's equation. The numerical values of α and β must now be obtained by fitting Equation 12 to actual penetration data. The best fit to the TTR data¹¹ (Figure 3) occurs for

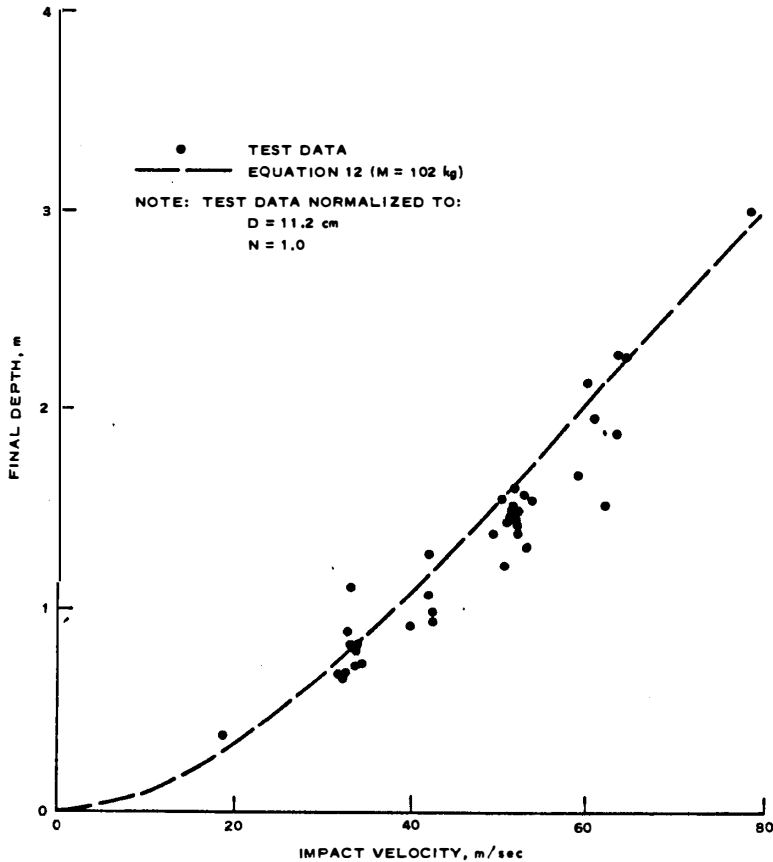


Figure 3. Correlation of TTR penetration data with Equation 12 for empirical determination of α and β

$$\alpha = 2.2 \times 10^6 \text{ N/m} \quad (16)$$

$$\beta = 2.8 \times 10^7 \text{ N/m}^3 \quad (17)$$

where Young's value of $S = 5.2$ has been assumed for the TTR Main Lake area.⁵ With α and β given in the units shown, Z can be obtained in metres from Equation 12 (in which the values of M , D , and V must be expressed in kilograms, metres, and metres per second, respectively).

13. The soil penetration analysis is now complete. Due to the presumption of a flat deceleration curve in the formulation of the equation of motion, the effect of the projectile mass (or weight) in

Equation 12 is slightly different from the effect in Young's equation. Close inspection of Equation 12 reveals that $Z \propto M$ as $MV^2 \rightarrow 0$ and that $Z \propto \sqrt{M}$ as $MV^2 \rightarrow \infty$. As the impact energy increases from zero, the M-dependence of Z gradually changes from linear to square root. In Young's equation, the M-dependence changes from linear (at $M \sim 1$ kg) to square root (at $M \geq 27$ kg), independent of the impact velocity. Figure 4 shows a comparison of Equation 12 with Young's equation (for $W \geq 27$ kg) and with normalized soil penetration data.

14. Figure 5 shows a comparison of calculated deceleration

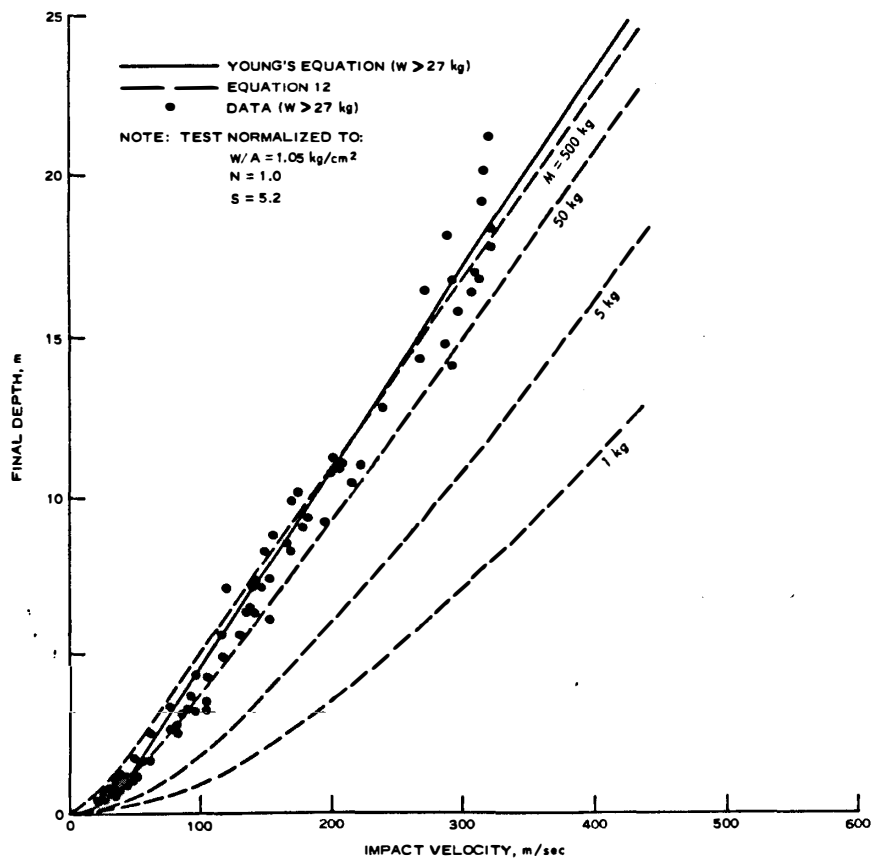


Figure 4. Comparison of Equation 12 with Young's equation and with normalized soil penetration data

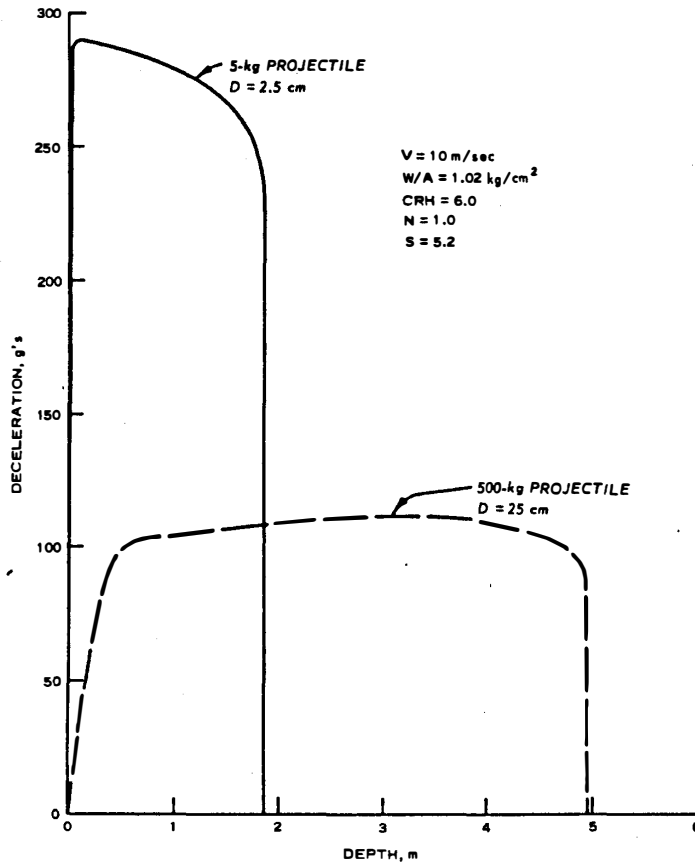


Figure 5. Comparison of calculated deceleration records in hypothetical soil target for impact velocity of 100 m/sec

curves* for a 500-kg, 25-cm projectile and a 5-kg, 2.5-cm projectile at an impact velocity of 100 m/sec. Figure 6 shows a similar comparison at 300 m/sec. In both cases, the lighter projectile incurs the higher deceleration, but the difference in deceleration between the two projectiles decreases as V increases.

* These results were obtained by numerical integration of Equation 11, accounting for the change in diameter during nose embedment. The projectiles have the same value of W/A .

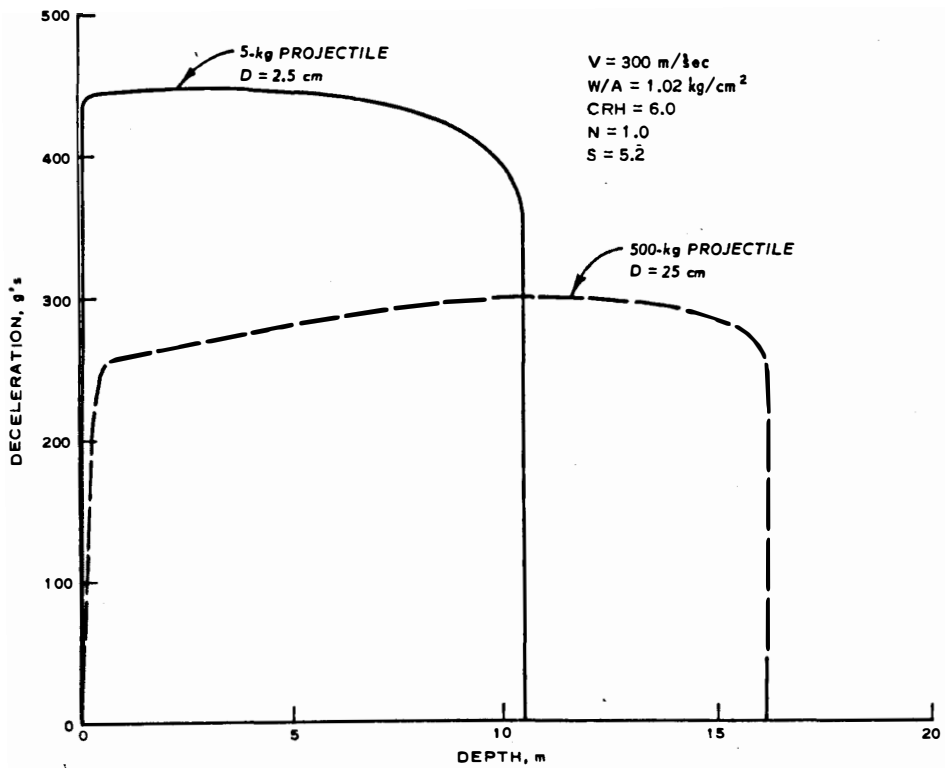


Figure 6. Comparison of calculated deceleration records in hypothetical soil target for impact velocity of 300 m/sec

PART III: ROCK PENETRATION ANALYSIS

15. Reference 12 documents an empirical equation for calculating final penetration depth in massive rock deposits. Expressed in dimensionless form,* the equation is:

$$\frac{\rho Z}{M/A} = 0.2V \sqrt{\frac{\rho}{Y}} \left(\frac{100}{RQD} \right)^{0.8} \quad (18)$$

where

ρ = mass density of the rock

Y = unconfined compressive strength of the intact rock

The RQD, originally proposed by Deere,⁹ is an index for the degree of fracturing of the rock (in situ) at a given site. Its value (in percent) is determined by a special core-logging procedure:

All solid pieces of core that are 10 cm long or longer are added up, and this length is called the modified core recovery. The modified core recovery is divided by the total length of core run, and the quotient multiplied by 100 percent is the value of the RQD.

16. Equation 18, like Young's equation, gives only the final depth of penetration; it does not predict the projectile motion after impact. This equation was obtained by curve-fitting data from rock penetration tests¹² in which ρ , Y , and RQD were all known. The data were somewhat scattered, however, and the linearity in V was chosen mainly for convenience of calculation.** A linear equation seemed to fit the overall data at least as accurately as other functions of V .

* Obviously, the values of ρ , Z , M , A , Y , and V must be expressed in compatible units if Equation 18 is to be dimensionless.

** Most of the scatter is due to uncertainty in the coefficient of penetrability from one target to the next. When several data exist for a single target, they usually exhibit (a) less scatter and (b) a weakly nonlinear relation between Z and V . However, when data from multiple targets are superposed, the apparent nonlinearity in V is lost in the scatter.

17. Existing deceleration records are too few to allow definitive statements about the shape of the deceleration curve in rock. Thus, the assumption of a flat deceleration record is not justified for rock as it was for soil. The formulation of the projectile equation of motion must rest on final-depth data alone.

18. Canfield and Clator⁸ have conducted a series of penetration tests in concrete, which is similar in some ways to intact (unjointed, unfractured) rock. The test results, obtained for 7.6- and 76-mm projectiles, suggest the following conclusions:

- a. The final depth is directly proportional to the projectile mass and inversely proportional to the square of the projectile diameter.
- b. The final depth increases linearly with impact velocity for $V > 300$ m/sec, but the curve has a nonzero intercept, indicating nonlinearity at low velocity.

A two-term equation of motion is needed to reproduce the trends in the concrete penetration data:

$$-M \frac{dv}{dt} = -Mv \frac{dv}{dz} = \frac{\pi}{4} D^2 (a' + b'v) \quad (19)$$

where a' and b' are coefficients independent of v and z but dependent on target properties. Neglecting the change in D during the nose-embedding process, the solution for the final depth is

$$z = \frac{4M}{\pi D^2} \left[\frac{v}{b'} - \frac{a'}{b'^2} \ln \left(1 + \frac{b'}{a'} v \right) \right] \quad (20)$$

Presuming that rock and concrete respond in much the same way to penetration, Equations 19 and 20 should also be applicable for rock, though the values of a' and b' may be different from those for concrete.

19. Figure 7 shows the concrete penetration data obtained by Canfield and Clator for a 76-mm projectile. Equation 22 fits these

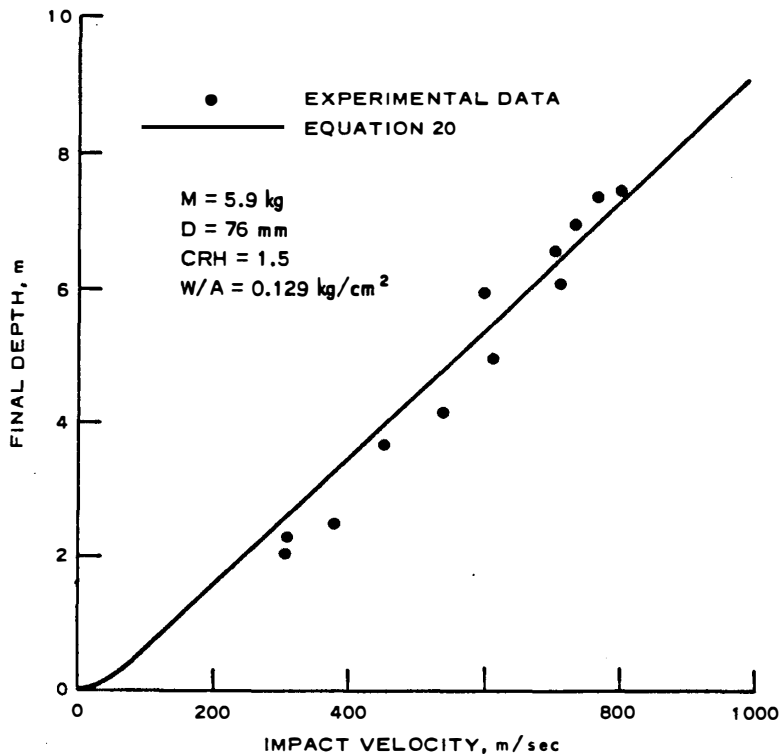


Figure 7. Correlation of penetration data for 5000-psi concrete with Equation 20 for empirical determination of a' and b'

data fairly well when a' and b' are given the following values:*

$$\text{concrete: } \begin{cases} a' = 1.6Y & (21) \\ b' = 3.6\sqrt{\rho Y} & (22) \end{cases}$$

In the Canfield and Clator tests, the unconfined compressive strength was 3.45×10^8 dyne/cm², and the density 2.88 gm/cm³.

20. Equations 19 and 20 are applicable for rock penetration (to at least the same degree as Equation 18) when Equations 21 and 22 are amended as follows:

* The values chosen for a' and b' do not produce a very good fit to the concrete data as such, but they do produce a good fit to superposed concrete and rock data.

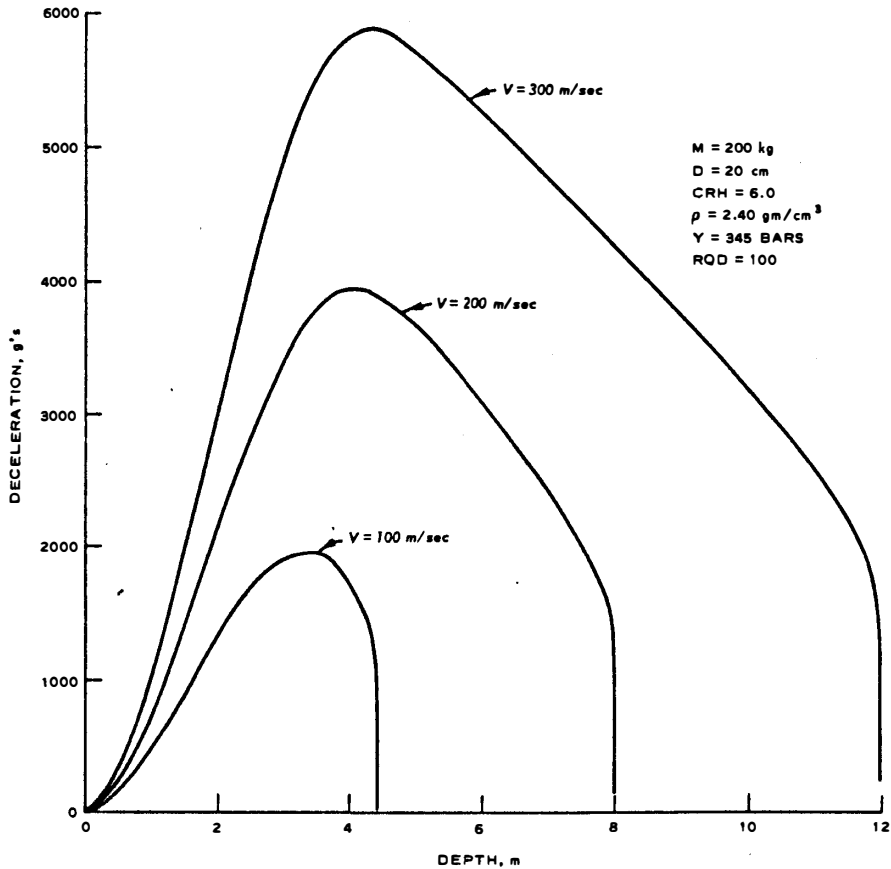


Figure 9. Calculated deceleration curves for 5000-psi concrete

for three different impact velocities. Due to the form of Equation 19 and the relative magnitudes of a' and b' , the maximum deceleration occurs at the point of nose embedment, with the minimum deceleration at the final penetration depth. If the coefficient of Y (Equation 21) were larger, and the coefficient of $\sqrt{\rho Y}$ (Equation 22) smaller, then the calculated deceleration curves would be flatter, and the relation between Z and V more nonlinear.

PART IV: LAYERED TARGET ANALYSIS

22. Few natural targets are uniform to any great depth, and it is not uncommon for earth penetrators to encounter abrupt changes in penetrability. This poses no special problem if the adjacent layers are similar materials (both soil or both rock), but a difficulty arises when a layer of rock overlies a layer of soil. A finite thickness of rock is more penetrable (per unit depth) than a half-space of the same rock, yet there do not exist enough rock-over-soil penetration data to formulate a quantitative model for the weakening of the rock near the interface. Aside from this shortcoming, the penetration analysis for layered targets is a logical extension of the work in Parts II and III.

Equation of Motion for Layered Targets

23. Upon considering the projectile equation of motion (Equations 11 and 19), it is convenient to introduce the quantity σ , which represents the resisting force per unit frontal area. This allows Equations 11 and 19 to be rewritten as

$$-M \frac{dv}{dt} = \frac{\pi}{4} D^2 \sigma \quad (25)$$

Whenever the projectile nose is in contact with two adjacent layers (Figure 10), Equation 25 is replaced by

$$-M \frac{dv}{dt} = \frac{\pi}{4} \left(D_1^2 - D_2^2 \right) \sigma_1 + \frac{\pi}{4} D_2^2 \sigma_2 \quad (26)$$

where

D_1, D_2 = maximum diameter in contact with layers 1 and 2, respectively

σ_1, σ_2 = value of σ in layers 1 and 2, respectively

Layered Soil Targets

24. Equation 26 is applicable for soil and rock layers alike, so

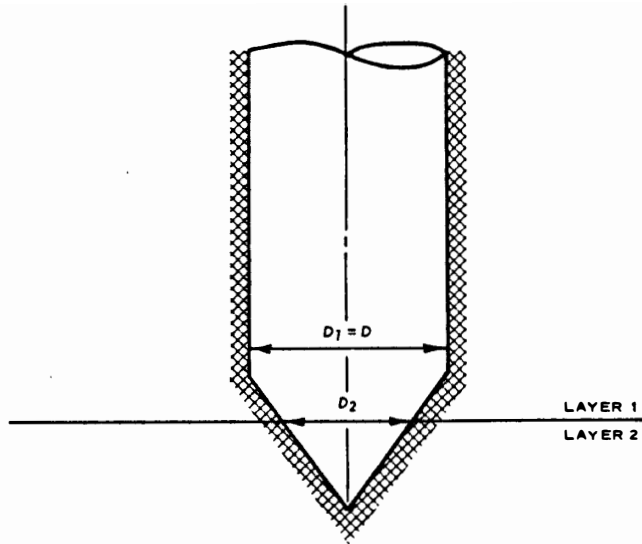


Figure 10. Projectile in contact with two layers at the same time

long as the definitions of σ_1 and σ_2 make Equation 26 consistent with Equations 11 and 19. For soil layers in particular, σ_1 and σ_2 must be defined such that Equation 26 reduces to

$$-M \frac{dv}{dt} = (a_1 + a_2) + (b_1 + b_2)v + (c_1 + c_2)z \quad (27)$$

where

$$a_1 = \frac{\alpha(D_1 - D_2)}{S_1 N} \quad (28)$$

$$a_2 = \frac{\alpha D_2}{S_2 N} \quad (29)$$

$$b_1 = \frac{D_1 - D_2}{S_1 N} \sqrt{\frac{3}{7} \beta M} \quad (30)$$

$$b_2 = \frac{D_2}{S_2 N} \sqrt{\frac{3}{7} \beta M} \quad (31)$$

$$c_1 = \frac{\beta(D_1^2 - D_2^2)}{S_1^2 N^2} \quad (32)$$

$$c_2 = \frac{\beta D_2^2}{S_2^2 N^2} \quad (33)$$

and S_1 and S_2 are the S-numbers in layers 1 and 2, respectively. With the coefficients defined in Equations 28-33, Equation 27 collapses to Equation 11 whenever $S_1 = S_2$. In order for Equation 26 to be consistent (for soil) with Equation 27, it then follows that

$$\sigma_1 = \frac{4}{\pi} \left(\frac{a_1 + b_1 v + c_1 z}{D_1^2 - D_2^2} \right) \quad (34)$$

$$\sigma_2 = \frac{4}{\pi} \left(\frac{a_2 + b_2 v + c_2 z}{D_2^2} \right) \quad (35)$$

where z is the depth of the nose tip, measured from the target surface. Figure 11 shows a numerically calculated deceleration curve for a hypothetical three-layer soil target.

Layered Rock Targets

25. In order to make Equation 26 consistent (for rock) with Equation 19, the definitions required for σ_1 and σ_2 are:

$$\sigma_1 = 1.6 Y_1 \left(\frac{RQD_1}{100} \right)^{1.6} + 3.6 v \sqrt{\rho_1 Y_1} \left(\frac{RQD_1}{100} \right)^{0.8} \quad (36)$$

$$\sigma_2 = 1.6 Y_2 \left(\frac{RQD_2}{100} \right)^{1.6} + 3.6 v \sqrt{\rho_2 Y_2} \left(\frac{RQD_2}{100} \right)^{0.8} \quad (37)$$

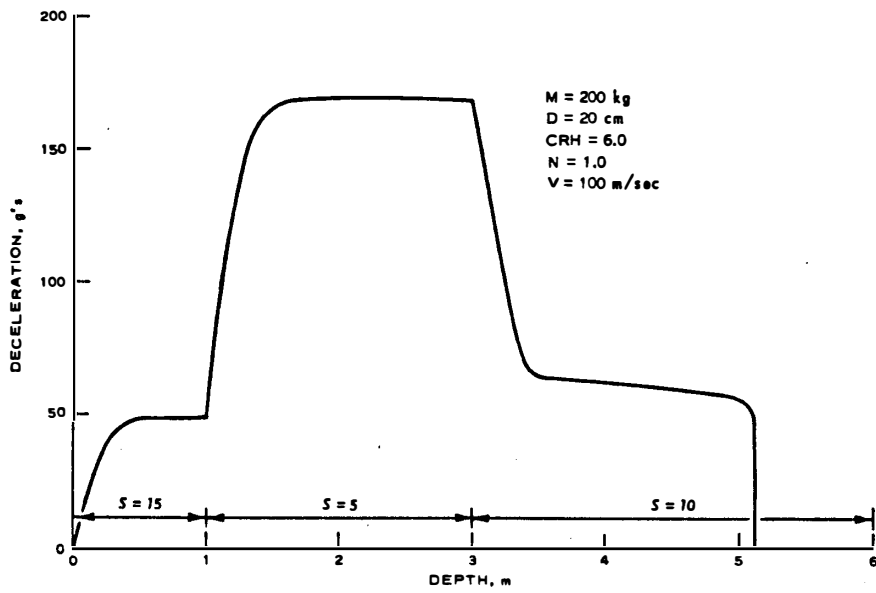


Figure 11. Calculated deceleration record for a hypothetical three-layer soil target

where the subscripts 1 and 2 designate the evaluation of ρ , Y , and RQD in layers 1 and 2, respectively. Figure 12 shows a numerically calculated deceleration record for a hypothetical three-layer rock target.

Composite Targets

26. Equation 26 is applicable for targets containing both soil and rock layers. Equations 34-35 and 36-37 define σ in the soil and rock layers, respectively. The total force on the projectile can be obtained by substituting the appropriate expressions for σ_1 and σ_2 into Equation 26. For example, if layer 1 is soil and layer 2 is rock, then σ_1 and σ_2 are given by Equations 34 and 37, respectively. Figure 13 shows a numerically calculated deceleration curve for a hypothetical soil/rock/soil target.

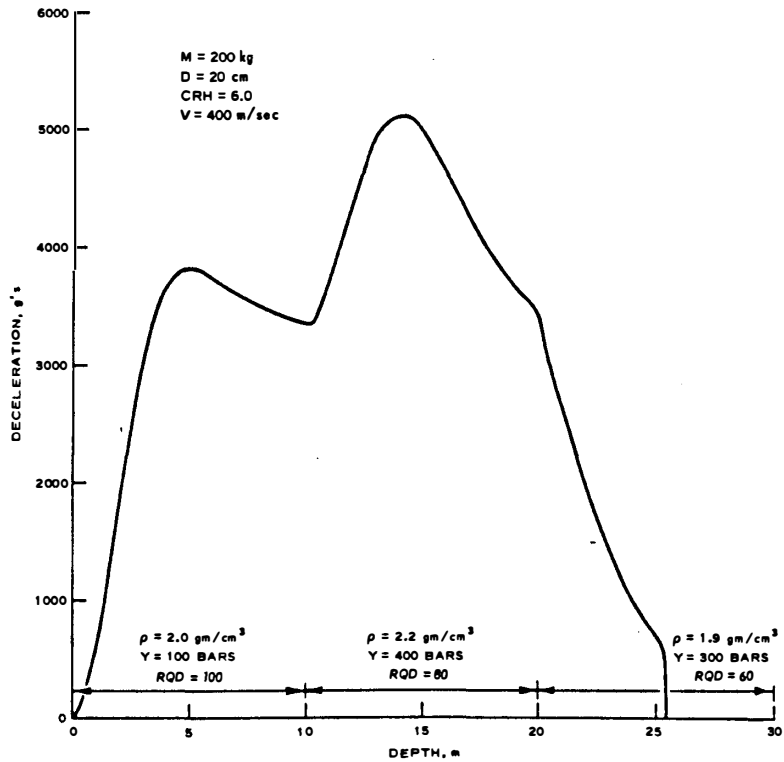


Figure 12. Calculated deceleration record for a hypothetical three-layer rock target

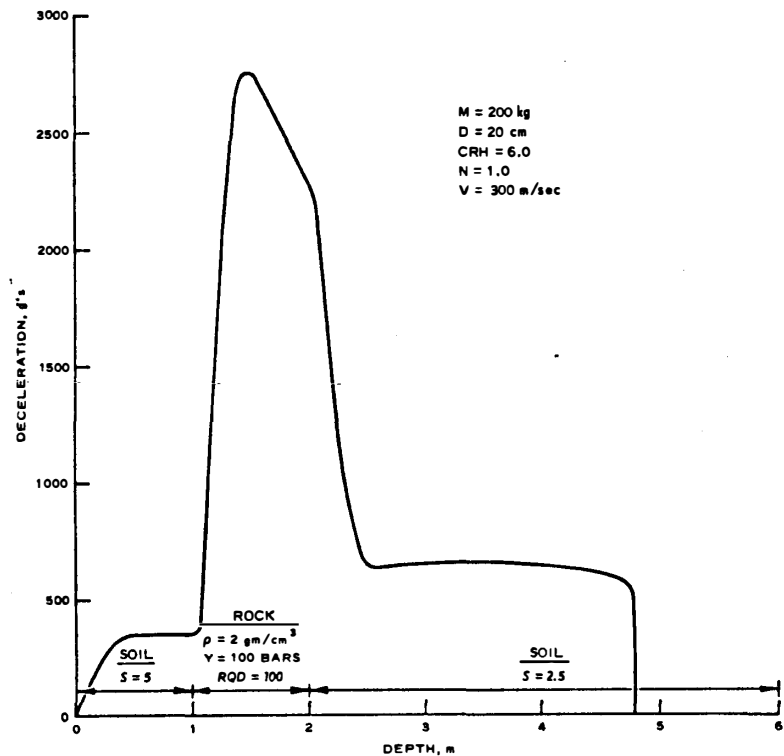


Figure 13. Calculated deceleration record for a hypothetical soil/rock/soil target

PART V: CONCLUSIONS

27. The soil penetration analysis (Part II) is a reexamination of the data originally used in the formulation of Young's equation. The projectile equation of motion (Equation 11) obtained therefrom (a) offers a means of calculating the projectile motion explicitly and (b) appears to clarify the effect of the projectile mass upon the final penetration depth. The accuracy of prediction is the same as for Young's equation: rigid-body deceleration and final depth ± 20 percent, when the S-number is known accurately.

28. The rock penetration analysis (Part III) is based on fewer data than the soil penetration analysis. Nevertheless, for high-quality rock ($RQD > 90$) in which the strength is known accurately, the final-depth predictions are usually accurate within ± 20 percent. For the same situation, predictions of peak rigid-body deceleration should be accurate at least within ± 50 percent. In order to improve upon this, more projectile deceleration records are needed to get a better understanding of (a) the general shape of the deceleration curve and (b) the relation between rock properties and rock penetrability.

29. The layered target analysis (Part IV) is a logical extension of Parts II and III. The equations therein should be about as accurate for layered targets as for unlayered targets, with the exception of rock layers over soil. In rock layers, the resistance to penetration decreases near a rock/soil interface, but the analysis does not account for this directly. For calculations involving thick rock layers over soil, the reduced penetrability can be approximated indirectly, however, by using a simple rule of thumb: Reduce the rock thickness by two or three projectile diameters, and increase the thickness of the underlying soil by the same amount.

REFERENCES

1. Bernard, R. S. and Hanagud, S. V., "Development of a Projectile Penetration Theory; Penetration Theory for Shallow to Moderate Depths," Technical Report S-75-9, Report 1, Jun 1975, U. S. Army Engineer Waterways Experiment Station, CE, Vicksburg, Miss.
2. Bernard, R. S., "Development of a Projectile Penetration Theory; Deep Penetration Theory for Homogeneous and Layered Targets," Technical Report S-75-9, Report 2, Feb 1976, U. S. Army Engineer Waterways Experiment Station, CE, Vicksburg, Miss.
3. Bernard, R. S. and Creighton, D. C., "Projectile Penetration in Earth Materials: Theory and Computer Analysis," Technical Report S-76-13, Nov 1976, U. S. Army Engineer Waterways Experiment Station, CE, Vicksburg, Miss.
4. Young, C. W., "The Development of Empirical Equations for Predicting Depth of an Earth-Penetrating Projectile," Development Report No. SC-DR-67-60, May 1967, Sandia Laboratories, Albuquerque, N. Mex.
5. _____, "Depth Prediction for Earth-Penetrating Projectiles," Journal, Soil Mechanics and Foundations Division, American Society of Civil Engineers, Vol 95, No. SM3, May 1969, pp 803-817.
6. _____, "Empirical Equations for Predicting Penetration Performance in Layered Earth Materials for Complex Penetrator Configurations," Development Report SC-DR-72-0523, Dec 1972, Sandia Laboratories, Albuquerque, N. Mex.
7. Rohani, B. et al., "Uncertainties in Predicting Earth Penetrator Performance in Inaccessible Geologic Targets," Miscellaneous Paper (in preparation), U. S. Army Engineer Waterways Experiment Station, CE, Vicksburg, Miss.
8. Canfield, J. A. and Clator, I. G., "Development of a Scaling Law and Techniques to Investigate Penetration in Concrete," Technical Report 2057, Aug 1966, U. S. Naval Weapons Laboratory, Dahlgreen, Va.
9. Deere, D. U., "Technical Description of Rock Cores for Engineering Purposes," Rock Mechanics and Engineering Geology, International Society of Rock Mechanics, Vol 1, No. 1, 1964, pp 16-22.
10. McNeill, R. L., "Rapid Penetration of Terrestrial Materials--The State of the Art," Proceedings, Conference on Rapid Penetration of Terrestrial Materials, Texas A&M University, Feb 1972, pp 11-125.
11. Young, C. W. and Ozanne, G. M., "Compilation of Low Velocity Penetration Data," Research Report SC-RR-66-306A, Jun 1966, Sandia Laboratories, Albuquerque, N. Mex.
12. Bernard, R. S., "Empirical Analysis of Projectile Penetration in Rock," Miscellaneous Paper S-77-16, Nov 1977, U. S. Army Engineer Waterways Experiment Station, CE, Vicksburg, Miss.

APPENDIX A: NOTATION

a,b,c	Coefficients in projectile equation of motion for soil (Equation 11)
a',b'	Coefficients in projectile equation of motion for rock (Equation 19)
A	Projectional cross-sectional area ($\pi D^2/4$)
CRH	Ogive caliber radius
D	Projectile diameter
g	Gravitational acceleration (9.8 m/sec^2)
K	Young's mass-scaling factor
L	Projectile nose length
M	Projectile mass
N	Projectile nose-performance coefficient
RQD	Rock Quality Designation
S	Young's penetrability index for soil
t	Time
v	Instantaneous velocity
V	Impact velocity, m/sec
W	Projectile weight, kg
Y	Unconfined compressive strength for rock and concrete
z	Instantaneous depth
Z	Final penetration depth, m
α, β	Coefficients in projectile equation of motion for soil (Equations 11, 13, 14, 15)
π	3.1416
ρ	Mass density for rock and concrete
σ	Resisting force per unit frontal area

Note: Subscripts 1 and 2 denote evaluation of a given quantity in layers 1 and 2, respectively (Figure 10).